Oxidation of Alkenes, Sulfides, Amines, and Phosphines with Peroxynitrous Acid: Comparison with Other Oxidants Such as Peroxyformic Acid and Dimethyldioxirane

Robert D. Bach,*[,1a] Mikhail N. Glukhovtsev,[1b] and Carlo Canepa[1c]

Contribution from the Department of Chemistry and Biochemistry, University of Delaware, Newark, Delaware 19716

Received July 25, 1997. Revised Manuscript Received November 24, 1997

Abstract: The oxidation reactions of ethylene, propene, dimethyl sulfide, trimethylamine, and trimethylphosphine with peroxynitrous acid have been studied computationally with the B3LYP, MP2, MP4, CISD, QCISD, and QCISD(T) levels of theory. The activation barriers for the alkene (ethylene and propene) epoxidations (18.4 and 15.5 kcal/mol at the QCISD(T)/6-31G*//QCISD/6-31G* level, respectively) and for the oxidations of dimethyl sulfide, trimethylamine, and trimethylphosphine (8.3, 4.6, and 0.5 kcal/mol at the QCISD(T)/6-31G*//B3LYP/6-311G** level, respectively) with peroxynitrous acid are similar to the barriers of their oxidations with peroxyformic acid and dimethyldioxirane, although these peroxides have very diverse O−O bond dissociation energies. Therefore, the feasibility of alkene epoxidation and the oxidations of methyl-substituted sulfides, amines, and phosphines by peroxynitrous acid should not differ significantly from those for peroxyformic acid and dimethyldioxirane. The transition structures for the epoxidation of ethylene and propene with peroxynitrous acid are symmetrical with equal or almost equal bond distances between the spiro oxygen and the carbons of the double bond. This symmetrical approach of the electrophilic oxygen is similar to that found for alkene epoxidations with peroxyformic acid. The geometries of the transition structures calculated at the QCISD and CISD levels are quite comparable to each other. The B3LYP calculated barriers for oxidations of alkenes, as well as sulfides, amines, and phosphines, are underestimated when compared with those calculated at the QCISD(T)//QCISD levels. The most economical and accurate protocol utilizes the B3LYP (for such "σ-donors" as sulfides, amines, and phosphines) or CISD geometries with barriers calculated at the QCISD(T) level.

1. Introduction

While peroxy acids have been in general use for nearly a century[2a,b] and substituted dioxiranes for two decades,[2c] the chemistry of peroxynitrous acid is still in its infancy.[2d] Consequently, we have not accumulated the great repository of experimental data that has shaped our mechanistic understanding of oxygen transfer reactions from peroxy acids and dioxiranes. The extent of experimental study on this class of oxidants is in part a reflection of their relative stability or shelf life. While peroxyacids can be stable for years, the half-life of dimethyldioxirane in solution is measured in days (see below) and that of peroxynitrous acid in seconds. It could be expected that the barrier heights for the oxidation reactions are related to the energy required for the O−O bond stretching and that the O−O bond dissociation energy for the oxidant governs the activation barrier. Peroxynitrous acid (HOONO) undergoes facile homolytic O−O bond fission to form OH and NO_2.[3] The O−O bond dissociation energy in HOONO calculated with G2 theory is 20.3 kcal/mol (D_o at 0 K) whereas the G2 calculated O−O bond energy in the peroxyformic acid is more than twice as great (46.9 kcal/mol).[4] Therefore, from an energetic perspective one could anticipate that peroxynitrous acid should be a much more effective oxidant than peroxyformic acid. At this time a comparative study of these three peroxides is particularly relevant and the use of high-level quantum theory provides a unique opportunity to examine the relative reactivity of these oxygen atom donors.

Peroxynitrite anion ($^-$OONO), a stable isolable peroxide formed by the provocative reaction of NO with O_2^-, is a potent oxidant that has been under great scrutiny by the biochemical community. Its conjugate acid, peroxynitrous acid, has an estimated lifetime of only 1−3 s at neutral pH,[5] but it can also play an important role in biochemical processes. Peroxynitrous acid acts as an oxidant in such various oxidation processes as, for example, the oxidation of ebselen (2-phenyl-1,2-benziso-selenazol-3(2*H*)-one) with further reduction of the selenoxide in cells to regenerate ebselen[6a] and the process of the killing of *Escherichia coli* by nitrite and hydrogen peroxide, which was observed in lactate.[6b] Peroxynitrous acid generated by the

(1) (a) E-mail rbach@udel.edu; WWW http://www.Udel.edu/chem/bach. (b) WWW http://Udel.edu/~mng. (c) On leave from the Universitá di Torino, Italy.

(2) (a) Prilezhaev, E. N. *Chem. Ber.* **1909**, *42*, 4811. (b) Bartlett, P. D. *Rec. Chem. Prog.* **1950**, *11*, 47. (c) Curci, R.; Fiorentino, M.; Troisi, L.; Edwards, J. O.; Pater, R. H. *J. Org. Chem.* **1980**, *45*, 4758. (d) Feldman, P. O.; Griffith, O. W.; Stuehr, D. J. *Chem. Eng. News* **1993**, *Dec 20*, 26.

(3) King, P. A.; Anderson, V. E.; Edwards, J. O.; Gustafson, G.; Plumb, R. C.; Suggs, J. W. *J. Am. Chem. Soc.* **1992**, *114*, 5430.

(4) Bach, R. D.; Ayala, P. Y.; Schlegel, H. B. *J. Am. Chem. Soc.* **1996**, *118*, 12758.

(5) Hughes, M. N.; Nicklin, H. G. *J. Chem. Soc. A* **1968**, 450.

(6) (a) Masumoto, H.; Sies, H. *Chem. Res. Toxicol.* **1996**, *9*, 262. (b) Kono, Y.; Shibata, H.; Adachi, K.; Tanaka, K. *Arch. Biochem. Biophys.* **1994**, *311*, 153.

S0002-7863(97)02518-3 CCC: $15.00
Published on Web 01/16/1998

reaction of nitrite with hydrogen peroxide either decomposes with the formation of nitrogen dioxide or reacts with lactate and produces secondary oxidants. These oxidants are responsible for the lactate-dependent killing of *E. coli*.[6b] Other examples are oxidations of amines, sulfides,[7a] and selenides.[7b] The three main mechanisms of these reactions are not well understood and are controversial. The first pathway involves homolytic O−O bond cleavage in peroxynitrous acid resulting in the formation of HO• and •NO2 as the initial reaction step.[8a] The second mechanism is a variation of the first; however, the oxidizing agent is thought to be an intermediate whose geometry is close to that of the transition structure for the isomerization of peroxynitrous acid into nitric acid.[8b,c] This intermediate, with a very weak O−O bond, is suggested to be amenable for hydroxyl radical-like oxidations with HOONO. The third mechanism involves a two-electron SN_2-like oxygen transfer from peroxynitrous acid to a nucleophile.[2]

The relatively short half-life of peroxynitrous acid hampers experimental studies of its reactions as an oxidizing agent. Therefore, theoretical methods can play a particularly useful role in describing the chemistry of peroxynitrous acid. We will consider the two-electron oxidations of such prototypical substrates as alkenes, sulfides, amines, and phosphines with peroxynitrous acid. This type of oxygen atom transfer reaction is similar to the corresponding oxidations with peroxyformic acid, where both experimental[9] and computational data are available.[10] The oxidative processes 1−4 of these key substrates can serve as models for the oxidizing activity of HOONO in biochemical transformations involving substrates with the same functional groups or fragments.[5,6] In this manner it can be ascertained whether biochemical reactions can share their basic mechanistic features with oxidations of the prototype molecules. Another mechanistic possibility for oxidations with HOONO is a single-electron process that involves the formation of a weakly bound radical pair, HO···ONO. This type of excited state intermediate is to be expected of reagents that have exceptionally low barriers to homolytic cleavage and can exhibit very diverse chemistries. We have considered this type of oxidative reaction elsewhere.[10i]

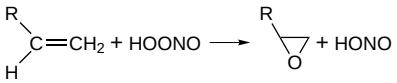

(1)

$$Me_2S + HOONO \longrightarrow Me_2S{-}O + HONO \quad (2)$$

$$Me_3N + HOONO \longrightarrow Me_3N{-}O + HONO \quad (3)$$

$$Me_3P + HOONO \longrightarrow Me_3P{-}O + HONO \quad (4)$$

High-level calculations of alkene epoxidation reactions with peroxyformic acid, HOO(C=O)H, which is isoelectronic with peroxynitrous acid (HOO(N=O), have indicated a symmetrical transition structure with C−O bond lengths that are either equal (ethylene) or close to each other (propene).[10] We have found that the B3LYP computational results for alkene epoxidation reactions with peroxyformic acid are in good agreement with the data of higher level calculations (QCISD(T)//QCISD, CASSCF, BD).[10g] This has allowed us to conclude that B3LYP calculations perform quite well for the transition structure geometries of epoxidation reactions. Both experimental and B3LYP data have recently appeared that also suggest that peracid epoxidations of alkenes proceed by a symmetrical transition structure.[11a]

Recently, the oxidations of ethylene, hydrogen sulfide, and ammonia with HO−ONO have been studied computationally[11b,c] with density functional theory (the B3LYP functional). However, an unsymmetrical geometry was reported for the transition structure for ethylene oxidation. Prior experience has taught us that electronically challenged oxidants such as HO−ONO should be very sensitive to the level of theory applied. As a consequence, key questions such as the type of transition structures and the magnitude of activation barriers still remain unclear. Furthermore, it has been established recently that reaction barriers for alkene epoxidations calculated with the B3LYP functional tend to be underestimated[10g] as are the barriers of some other reactions (e.g. SN_2 reactions, radical reactions).[12] Do transition structures and activation barriers in alkene epoxidations with peroxynitrous acid differ from those in oxidations with peroxyformic acid? And if so, to what can we attribute these differences? We address these questions in the present study and report comparative results of calculations carried out at the QCISD(T), QCISD, CISD, and MP2 levels of theory.

2. Computational Method

Ab initio calculations[13] were carried out with the GAUSSIAN-94 system of programs.[14] Geometries were optimized with analytic gradient techniques[15] at various levels of electron correlation: MP2, CISD, and QCISD (see, e.g., ref 13). We have also used density functional theory (DFT) with the three-parameter hybrid functional of Becke (B3)[16a] combined with the Lee, Yang, and Parr (LYP)[16b] correlation functional (B3LYP).[17] Zero point energies computed at the B3LYP/6-311G** level were scaled by 0.9806.[18] Throughout this paper lengths are in angstroms and bond angles are in degrees.

(7) (a) Pryor, W. A.; Jin, X.; Squadrito, G. L. *Proc. Natl. Acad. Sci. U.S.A.* **1994**, *91*, 11173. (b) Padmaja, S.; Squadrito, G. L.; Lemercier, J. N.; Cueto, R.; Pryor, W. A. *Free Radical Biol. Med.* **1996**, *21*, 317.

(8) (a) Mahoney, L. R. *J. Am. Chem. Soc.* **1970**, *92*, 5262. (b) Koppenol, W. H.; Moreno, J. J.; Pryor, W. A.; Ischiropoulos, H.; Beckman, J. S. *Chem. Res. Toxicol.* **1992**, *5*, 834. (c) A nonplanar transition structure for the isomerization of peroxynitrous acid into nitric acid was found at the HF/6-31G* level.[8d] However, our calculations have shown that the corresponding RHF solution is triplet unstable and that further geometry optimizations of this transition structure at a correlated level (B3LYP, MP2, QCISD) reveal that it does not correspond to a stationary point. (d) Cameron, D. R.; Borrajo, A. M. P.; Bennett, B. M.; Thatcher, G. R. J. *Can. J. Chem.* **1995**, *73*, 1627.

(9) (a) Lynch, B. M.; Pausacker, K. H. *J. Chem. Soc.* **1955**, 1525. (b) Schwartz, N. N.; Blumbergs, J. H. *J. Org. Chem.* **1964**, *29*, 1976. (c) Vilka, M. *Bull. Soc. Chim. Fr.* 1959, 1401. (d) Renolen, P.; Ugelstad, J. *J. Chim. Phys.* **1960**, *57*, 634. (e) House, H. O.; Ro, R. S. *J. Am. Chem. Soc.* **1958**, *80*, 2428. (f) Ogata, Y.; Tabushi, I. *J. Am. Chem. Soc.* **1961**, *83*, 3440, 3444. (g) Curci, R.; DiPrete, R. A.; Edwards, J. O.; Modena, G. *J. Org. Chem.* **1970**, *35*, 740.

(10) (a) Bach, R. D.; Willis, C. L.; Domagals, J. M. In *Applications of MO theory in Organic Chemistry*; Csizmadia, I. C., Ed.; Elsevier: Amsterdam, 1977; Vol. 2, p 221. (b) Bach, R. D.; Andrés, J. L.; Davis, F. *J. Org. Chem.* **1992**, *57*, 613. (c) Bach, R. D.; Owensby, A.; González, C.; Schlegel, H. B. *J. Am. Chem. Soc.* **1991**, *113*, 2338. (d) Bach, R. D.; Su, M.-D.; Schlegel, H. B. *J. Am. Chem. Soc.* **1994**, *116*, 5379. (e) Bach, R. D.; Andrés, J. L.; Owensby, A.; Schlegel, H. B. *J. Am. Chem. Soc.* **1992**, *114*, 7207. (f) Bach, R. D.; Winter, J. E.; McDouall, J. J. W. *J. Am. Chem. Soc.* **1995**, *117*, 8586. (g) Bach, R. D.; Glukhovtsev, M. N.; Gonzalez, C.; Marquez, M.; Estevez, C. M.; Baboul, A. G.; Schlegel, H. B. *J. Phys. Chem. A* **1997**, *101*, 6092. (h) Baboul, A. G.; Schlegel, H. B.; Glukhovtsev, M. N.; Bach, R. D. *J. Comput. Chem*. In press. (i) Glukhovtsev, M. N.; Canepa, C.; Bach, R. D. *J. Am. Chem. Soc*. Submitted for publication.

(11) (a) Singleton, D. A.; Merrigan, S. R.; Liu, J.; Houk, K. N. *J. Am. Chem. Soc.* **1997**, *119*, 3385. (b) Houk, K. N.; Condroski, K. R.; Pryor, W. A. *J. Am. Chem. Soc.* **1996**, *118*, 13002. (c) Houk, K. N.; Liu, J.; DeMello, N. C.; Condroski, K. R. *J. Am. Chem. Soc.* **1997**, *119*, 10147.

(12) (a) Glukhovtsev, M. N.; Bach, R. D.; Pross, A.; Radom, L. *Chem. Phys. Lett*. **1996**, *260*, 558. (b) Torrent, M.; Duran, M.; Solà, M. *J. Mol. Struct. (THEOCHEM)* **1996**, *362*, 163. (c) Jursic, B. S. *J. Chem. Phys.* **1996**, *104*, 4151. (d) Durant, J. L. *Chem. Phys. Lett.* **1996**, *256*, 595. (e) Thiimmel, H. T.; Bauschlicher, C. W. *J. Phys. Chem. A* **1997**, *101*, 1788.

(13) (a) Hehre, W. J.; Radom, L.; Schleyer, P. v. R.; Pople, J. A. *Ab Initio Molecular Orbital Theory*; Wiley: New York, 1986. (b) Raghavachari, K. *Annu. Rev. Phys. Chem.* **1991**, *42*, 615. (c) Raghavachari, K.; Anderson, J. B. *J. Phys. Chem.* **1996**, *100*, 12960.

Table 1. Relative Energies (kcal/mol) of the Lowest Energy Conformations of HOONO Calculated at Various Computational Levels

conformation	B3LYP/ 6-311G**	G2[b]	CBS-APNO[a]	QCISD(T)/6-31G*// CISD/6-31G*
cis-cis[c]	0	0	0	0
cis-perp	1.2	1.2	1.9	1.2
trans-perp	3.6[d]	3.1	3.8	3.7

[a] Referemce 19. [b] Reference 20. [c] The geometry of cis-cis conformation optimized at the QCISD, CISD, B3LYP, and MP2 levels of theory is shown in Figure 1. [d] The B3LYP/6-31G* calculations give a relative energy of 4.7 kcal/mol.

3. Results and Discussion

Peroxynitrous Acid. While HF/6-31G*, HF/6-31G**, and CCSD/6-311++G** calculations have led to a HOONO cis conformation that has a perpendicular orientation of the OH bond (cis-perp) and is lower (1.2 kcal/mol at the CCSD/6-311++G** level) in energy than the planar cis-cis conformation,[19] the G2[20] and CBS-APNO[19] calculations show a planar cis-cis conformation of HOONO as its most stable form. Our QCISD(T)/6-31G*//CISD/6-31G* and B3LYP/6-311G** calculations have also indicated that the planar cis-cis conformation of HOONO (**1**) is the most stable (Table 1). Therefore, we compute activation barriers with respect to the isolated HOONO planar cis-cis conformation and the substrate. It is notable that the relative energies for HOONO calculated at the B3LYP/6-311G** level are close to those computed at higher levels of theory (Table 1). The HOONO geometry **1** optimized at the B3LYP/6-311G** level does not differ significantly from the geometries found with the CISD and QCISD/6-31G* methods except that the B3LYP calculation affords a larger H−O1 distance (Figure 1). An RHF → UHF (triplet) instability[21] was reported for sodium peroxynitrite, ONOONa.[22] We have found that while the RHF solution at the B3LYP/6-311G** geometry of **1** is also triplet unstable (the lowest eigenvalue of the stability matrix is −0.00186 hartree), the B3LYP solution is both singlet and triplet stable (the lowest eigenvalue of the triplet stability matrix is 0.08314 hartree). Thus, the B3LYP method appears to be capable of providing a reliable description of the electronic structure and geometry of HOONO. This agrees with earlier findings that the performance of the B3LYP functional in calculations of nitrogen peroxides[23a] and nitrogen oxides[23b] is acceptable.

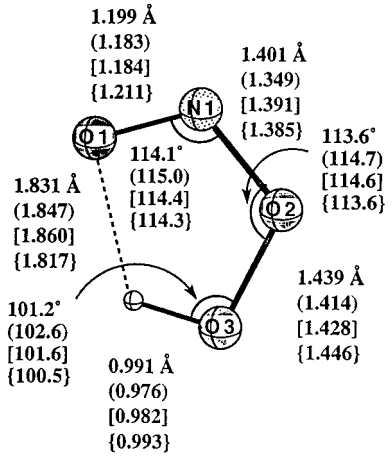

1 C_s

Figure 1. The geometry of the lowest energy (cis-cis) conformation of peroxynitrous acid (**1**) calculated at QCISD/6-31G*, CISD/6-31G* (in parentheses), B3LYP/6-311G** (in square brackets), and MP2(full)/6-31G* (in curly brackets) computational levels.

Epoxidation of Ethylene and Propene. Both MP2 and B3LYP calculations resulted in unsymmetrical transition structures for ethylene and propene epoxidations with peroxynitrous acid (Figure 2). The difference in the C−O bond distances between the ethylene carbons and the spiro-oxygen in **2b** is 0.393 Å at the B3LYP/6-311G** level and even larger (0.575 Å) at the MP2 level. The geometry optimization at the B3LYP/6-311+G(3df,2p) level also gave unsymmetrical transition structures with geometrical parameters close to those calculated with the 6-311G** basis. The geometry optimizations carried out at the CISD and QCISD levels, however, led to an almost symmetrical transition structure for ethylene (**2a**, the differences in the C−O bond distances are 0.001 Å at both the QCISD/6-31G* and CISD/6-31G* levels, Figure 2) and propene (**3a**, Figure 3). The harmonic frequencies calculated for **2a** at the CISD/6-31G* level confirm that it is a transition structure (one negative eigenvalue of the Hessian). Thus, the nature of the transition structures differs significantly at the MP2 and B3LYP levels relative to those calculated at the CISD/6-31G* and QCISD/6-31G* levels. Contrariwise, the B3LYP calculations of ethylene and propene epoxidation reactions with peroxyformic acid give symmetrical-type transition structures in agreement with the QCISD and CISD results.[10g]

Both the RHF and RB3LYP wave functions for the transition structure (at the B3LYP/6-311G** geometry) for the epoxidation of ethylene with HOONO suffer from a triplet instability (the negative eigenvalues of the stability matrix $({}^t\lambda_+)$[21] are −0.08401 and −0.00877 hartrees respectively). In contrast, the stability analysis of the RB3LYP solution for the transition structure of the epoxidation of ethylene with peroxyformic acid is triplet stable and led to a symmetrical transition structure.[10g] The RHF wave function for this transition structure possesses a triplet instability[21] and an unsymmetrical transition structure of the epoxidation of ethylene with peroxyformic acid has been found

(14) Frisch, M. J.; Trucks, G. W.; Schlegel, H. B.; Gill, P. M. W.; Johnson, B. G.; Robb, M. A.; Cheeseman, J. R.; Keith, T. A.; Peterson, G. A.; Montgomery, J. A.; Raghavachari, K.; Al-laham, M. A.; Zakrzewski, V. G.; Ortiz, J. V.; Foresman, J. B.; Cioslowski, J.; Stefanov, B. B.; Nanayakkara, A.; Challacombe, M.; Peng, C. Y.; Ayala, P. Y.; Wong, M. W.; Replogle, E. S.; Gomperts, R.; Andres, J. L.; Martin, R. L.; Fox, D. J.; Binkley, J. S.; DeFrees, D. J.; Baker, J.; Stewart, J. J. P.; Head-Gordon, M.; Gonzalez, C.; Pople, J. A. GAUSSIAN-94, Gaussian Inc.: Pittsburgh, PA, 1995.

(15) (a) Schlegel, H. B. *J. Comput. Chem.* **1982**, *3*, 214. (b) Schlegel, H. B. *Adv. Chem. Phys.* **1987**, *67*, 249. (c) Schlegel, H. B. In *Modern Electronic Structure Theory*; Yarkony, D. R., Ed.; World Scientific: Singapore, 1995; p 459.

(16) (a) Becke, A. D. *Phys. Rev. A* **1988**, *37*, 785. (b) Lee, C.; Yang, W.; Parr, R. G. *Phys. Rev.* **1988**, *B41*, 785.

(17) (a) Becke, A. D. *J. Chem. Phys.* **1993**, *98*, 5648. (b) Stevens, P. J.; Devlin, F. J.; Chablowski, C. F.; Frisch, M. J. *J. Phys. Chem.* **1994**, *98*, 11623.

(18) Scott, A. P.; Radom, L. *J. Phys. Chem.* **1996**, *100*, 16502.

(19) Tsai, H.-H.; Hamilton, T. P.; Tsai, J.-H. M.; van der Woerd, M.; Harrison, J. G.; Jablonsky, M. J.; Beckman, J. S.; Koppenol, W. H. *J. Phys. Chem.* **1996**, *100*, 15087.

(20) McGrath, M. P.; Rowland, F. S. *J. Phys. Chem.* **1994**, *98*, 1061.

(21) For the Hartree-Fock instabilities, see, for example: (a) Seeger, R. R.; Pople, J. A. *J. Chem. Phys.* **1976**, *65*, 265. (b) Chambaud, G.; Levy, B.; Millie, P. *Theor. Chim. Acta* **1978**, *48*, 103. (c) Glukhovtsev, M. N.; Mestechkin, M. M.; Minkin, V. I.; Simkin, B. Ya. *Zh. Strukt. Khim. (USSR)* **1982**, *23*, 14. (d) Schlegel, H. B.; McDouall, J. J. W. In *Computational Advances in Organic Chemistry: Molecular Structure and Reactivity*; Ögretir, C., Csizmadia, I. G., Eds.; Kluwer: Dordrecht, 1991; p 167. (e) Chen, W.; Schlegel, H. B. *J. Chem. Phys.* **1994**, *101*, 5957.

(22) Tsai, H.-H.; Hamilton, T. P.; Tsai, J.-H. M.; Harrison, J. G.; Beckman, J. S. *J. Phys. Chem.* **1996**, *100*, 6942.

(23) (a) McKee, M. L. *J. Am. Chem. Soc.* **1995**, *117*, 1629. (b) Jursic, B. S. *Int. J. Quantum Chem.* **1996**, *58*, 41.

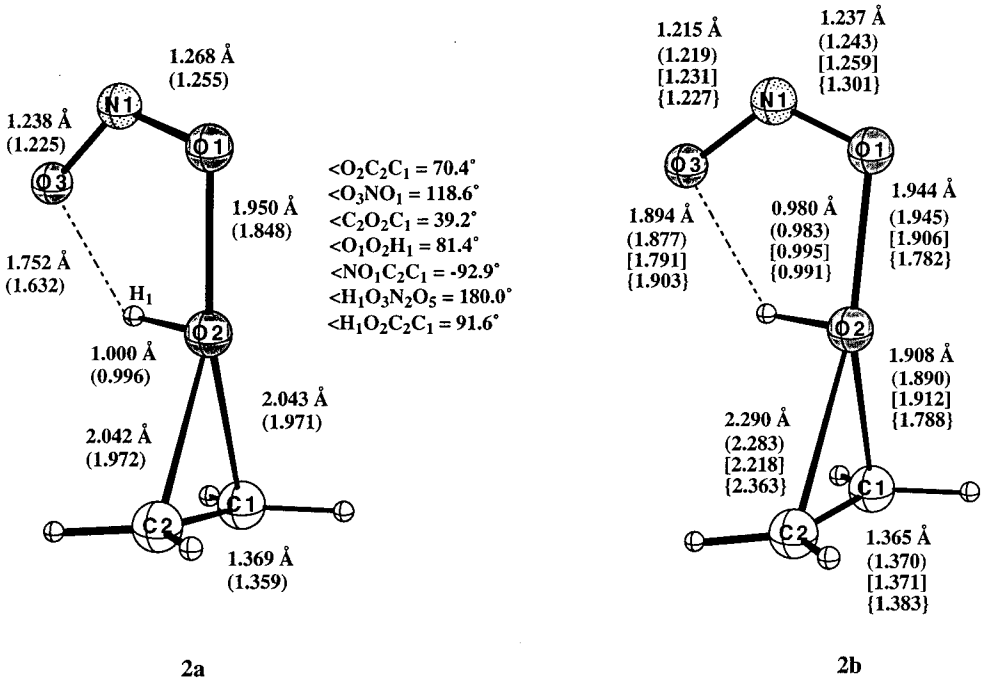

Figure 2. Geometrical parameters of symmetrical transition structure **2a** for ethylene epoxidation with peroxynitrous acid optimized at the QCISD/6-31G* and CISD/6-31G* (values are in parentheses) levels and unsymmetrical transition structure **2b** resulting from the geometry optimizations at the B3LYP/6-311+G(3df,2p), B3LYP/6-311G** (values in parentheses), B3LYP/6-31G* (values in square brackets), and MP2(full)/6-31G* (in curly brackets) levels. The full set of QCISD/6-31G* geometrical parameters for **2a** is given as the most reliable data.

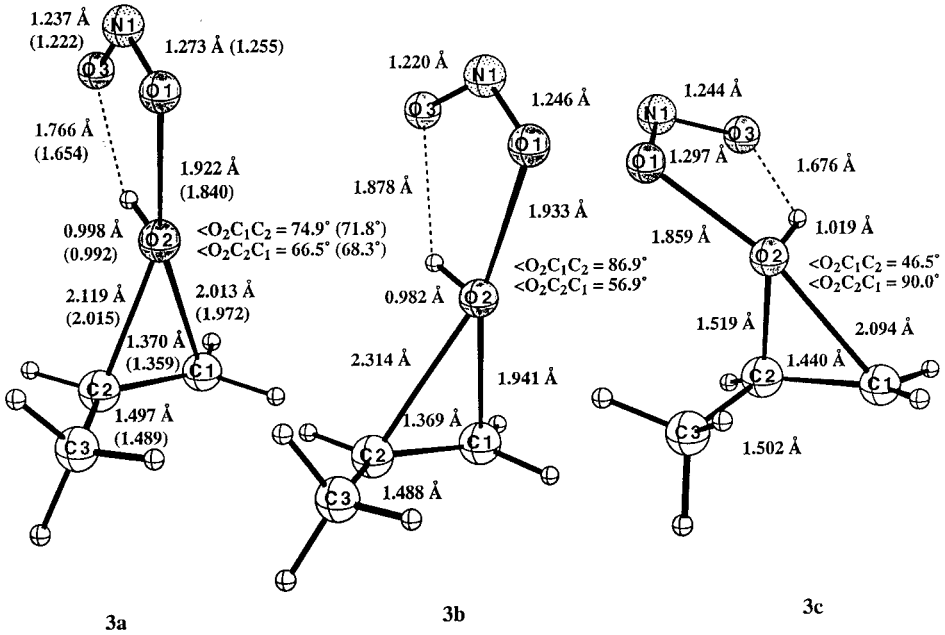

Figure 3. Geometrical parameters of the nearly symmetrical transition structure **3a** for ethylene epoxidation with peroxynitrous acid optimized at the QCISD/6-31G* and CISD/6-31G* (values are in parentheses) levels and unsymmetrical transition structures **3b** and **3c** resulting from the geometry optimizations at the B3LYP/6-311G** and MP2(full)/6-31G* levels, respectively. The activation barriers are listed in Table 3.

at the MP2 level.[10f] Analogously, the MP2/6-31G* optimization leads to an unsymmetrical transition structure (**2b**) for the epoxidation of ethylene with HOONO (Figure 2) and the corresponding RHF solution exhibits a triplet instability ($^t\lambda_+ = -0.05467$ hartree). Therefore, we suggest that the triplet instability of both RB3LYP and RHF solutions is responsible for the difference in the symmetry of the ethylene−peroxynitrous acid transition structure. In general, an unsymmetrical transition structure with alkene epoxidation when an alternative symmetrical structure is possible appears to be associated with an unstable wave function.

For the epoxidation of propene with HOONO, both the QCISD and CISD calculations result in a Markovnikov-type transition structure, where the electrophile is slightly skewed toward the least substituted carbon, with a small difference in the bond lengths between the spiro-oxygen and the double-bond carbons (0.106 and 0.043 Å, respectively; Figure 3). The B3LYP calculations also lead to an unsymmetrical Markovnikov-type transition structure (**3b**). However, the MP2/6-31G* geometry optimization results in a anti-Markovnikov-type structure (**3c**) (Figure 3). The latter exhibits a rather short developing bond between the spriro-oxygen and one of the

Table 2. Barrier Heights (kcal/mol) for the Epoxidation of Ethylene with Peroxynitrous Acid Calculated at Various Computational Levels

method	B3LYP/6-311G** geometry[a]	MP2(full)/6-31G* geometry[a]	CISD/6-31G* geometry	QCISD/6-31G* geometry
B3LYP/6-311G**	12.8[b] (13.4)[c]	15.7		
MP2(full)/6-31G*	19.9	15.4		
MP4SDTQ	15.1	15.2	16.7	16.8
QCISD	25.2	27.7	25.4	24.7
QCISD(T)	17.4	19.6	19.3	18.4[d]

[a] B3LYP, CISD, QCISD, and MP2 optimized geometries of the transition structures for the epoxidation of ethylene with peroxynitrous acid (**2a** and **2b**, respectively) are shown in Figure 2. [b] The B3LYP/6-311+G(3df,2p)//B3LYP/6-311+G(3df,2p) calculations give a barrier of 14.8 kcal/mol. The transition structure geometry optimized at this level (**2b**) is given in Figure 2. For the ethylene oxidation with peroxyformic acid, the barrier calculated at the B3LYP/6-311+G(3df,2p)//B3LYP/6-311+G(3df,2p) level (16.9 kcal/mol) is also slightly higher than that computed at the B3LYP/6-31G* level of theory (14.1 kcal/mol).[10g] [c] The barrier with the ZPE corrections calculated at the B3LYP/6-311G** level. [d] The barriers calculated at the CCSD(T)/6-31G* and BD(T)/6-31G* levels using the QCISD/6-31G* geometries are 18.4 and 19.9 kcal/mol, respectively. The barrier is 19.1 kcal/mol at the CCSD(T)/6-311G**//QCISD/6-31G* level.

Table 3. Barrier Heights (kcal/mol) for the Epoxidation of Propene with Peroxynitrous Acid Calculated at Various Computational Levels

method	B3LYP/6-311G** geometry[a]	MP2(full)/6-31G* geometry[a]	CISD/6-31G* geometry[a]	QCISD/6-31G geometry[a]
B3LYP/6-311G**	10.2 (11.0)[b]			
MP2(full)/6-31G*		8.8		
MP4SDTQ	12.6	3.4	13.5	13.1
QCISD	22.5	20.1	22.8	22.0
QCISD(T)	15.1	13.4[c]	16.5	15.5

[a] B3LYP, MP2, CISD, and QCISD optimized geometries of the transition structures for the epoxidation of propene with peroxynitrous acid (**3a**−**c**) are shown in Figure 3. [b] The barrier value calculated at the B3LYP/6-31G*/B3LYP//6-31G* level is given in parentheses. [c] A large difference between the QCISD(T)/6-31G*//MP2/6-31G* and MP4/6-31G*//MP2/6-31G* barriers also has been found for the epoxidation of ethylene with dimethyldioxirane.[10g]

double bond carbons (1.519 Å). The same behavior was observed in the peroxy acid epoxidation of propene where two first-order saddle points corresponding to these two transition structures were located. Attempts of the optimization of **3c** with the B3LYP method have led eventually to **3b**. Likewise in the transition structures for ethylene epoxidation, both the RHF and B3LYP wave functions for **3b** are triplet unstable.[24]

The CCSD(T)/6-31G* and BD(T)/6-31G* barriers for the ethylene epoxidation with HOONO calculated with the QCISD/6-31G* optimized geometries are 18.4 and 19.9 kcal/mol, respectively. The BD(T) barrier coincidently is the same as the BD(T)/6-31G*//QCISD/6-31G* barrier for the epoxidation of ethylene with peroxyformic acid.[10g] The CCSD(T)/6-31G*//CCSD/6-31G* (19.4 kcal/mol)[10g] and CCSD(T)/6-31G*//QCISD/6-31G* barriers for both reactions are also close to each other. A basis set extension to the 6-311G** basis set does not result in a significant change of the CCSD(T) barrier for the C_2H_4 + HOONO reaction (19.1 kcal/mol).

The B3LYP calculations with the 6-311G** and 6-31G* basis sets lead to transition structure geometries and activation barrier values (12.8 and 13.4 kcal/mol, respectively) for the epoxidation of ethylene (Figure 2, Table 2) that are quite similar. The basis set extension to the 6-311+G(3df,2p) basis set results in a modest increase in the barrier to 14.8 kcal/mol. These B3LYP barrier heights are, however, underestimated when compared with the QCISD(T)//QCISD and QCISD(T)//CISD barriers (18.4 and 19.3 kcal/mol, respectively) (Table 2). The B3LYP barrier is also underestimated for the epoxidation of propene with HOONO (a barrier of 10.2 kcal/mol, Table 3) when compared to the QCISD(T)/6-31G*//QCISD/6-31G* barrier (15.5 kcal/mol). A similar trend of the B3LYP functional in underestimating the activation barrier has been found for the alkene epoxidation reactions with peroxyformic acid.[10g] The MP4 and MP2/6-31G* barriers for the epoxidation of ethylene and propene with HOONO are also underestimated. The importance of the triples corrections is manifested by an overestimation of the barriers calculated at the QCISD level relative to the QCISD(T) values. Both the MP2//MP2/6-31G* and MP4SDTQ//MP2/6-31G* barriers for the epoxidation of ethylene with peroxynitrous acid (15.4 and 15.2 kcal/mol, respectively) are underestimated but to a lesser extent than the B3LYP barriers.

The QCISD(T), QCISD and MP4SDTQ barriers calculated with the QCISD/6-31G* and CISD/6-31G* optimized geometries, respectively, are in good agreement with each other (Tables 2 and 3). A similar trend has been found for the calculated barriers of alkene epoxidations with peroxyformic acid.[10g] The QCISD(T)/6-31G* barriers for the epoxidation of ethylene with HOO(C=O)H calculated at the QCISD and CISD/6-31G* geometries are 18.8 and 19.4 kcal/mol, respectively. This allows us to conclude that CISD optimized geometries can be employed for higher level single point calculations of alkene epoxidation reactions with peroxynitrous and peroxyformic acids[25] although calibration calculations may be necessary for a particular case. As noted for the epoxidation of alkenes with HOO(C=O)H,[10g] the activation barriers calculated at the QCISD(T)/6-31G* level with the B3LYP optimized geometries are close to those computed at the more computer-time demanding QCISD(T)/6-31G*//QCISD/6-31G* and QCISD(T)/6-31G*//CISD/6-31G* levels of theory. It was gratifying to observe the same trend with HOONO notwithstanding the fact that the B3LYP and QCISD (or CISD) transition state geometries differ from each other to a much greater extent than those for epoxidations with peroxyformic acid.

Similar to the relationship between the barriers for the epoxidation of ethylene and propene with peroxyformic acid,[10g] the activation barrier for the epoxidation of propene with peroxynitrous acid is lower than that for the epoxidation of ethylene (Figures 2 and 3) reflecting the rate increase that

(24) The negative eigenvalues ($^t\lambda_+$) of the stability matrix are −0.02242 and −0.00207 hartree, respectively; the smaller absolute value of $^t\lambda_+$ for the B3LYP solution indicates that the triplet instability for this wave function is less than that for the RHF wave function.

(25) The CISD method is not size consistent[13a] and, as a consequence, the calculated reaction barriers may be incorrect. Therefore, we recommend using the CISD optimized geometries provided that the barrier values are calculated at the QCISD(T) level.

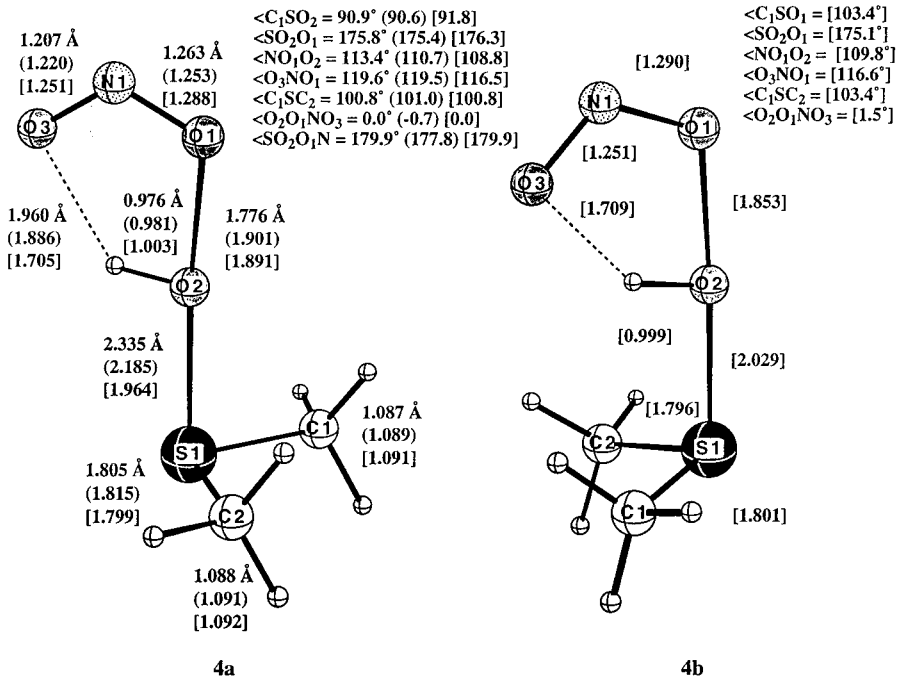

Figure 4. Geometrical parameters of transition structures **4a** and **4b** for the oxidation of dimethyl sulfide with peroxynitrous acid optimized at the B3LYP/6-311G** and MP2(full)/6-31G* (in parentheses) levels. The calculated activation barriers are shown in Table 4.

typically accompanies each additional alkyl substituent on the double bond.[26]

The most pronounced difference between the transition structure geometry[2a] and the geometries of the isolated reactants is the elongation of the O_1-O_2 bond by 0.510 Å at the QCISD/6-31G* level (0.420 Å at the CISD/6-31G* level), which is accompanied by a lengthening of the $N-O_1$ bond (Figures 1 and 2). Similar changes in the O−O bond length have been found for the transition structure in the epoxidation of ethylene with peroxyformic acid and discussed by us in terms of the electron density transfer from the π-orbital of the double bond to the antibonding σ^*-orbital of the O_1-O_2 bond.[10g] The distances between the oxygen (O_3) and hydrogen atoms participating in the formation of the hydrogen bond decrease in **2a** and **3a** when compared with that in **1** (by 0.079 and 0.065 Å, respectively, for the QCISD/6-31G* optimized structures, Figures 1−3).

Oxidations of Dimethyl Sulfide, Trimethylamine, and Trimethylphosphine. We have considered a methyl-substituted sulfide, amine, and phosphine as a prototypical nucleophile rather than the unsubstituted parent species because generalizing conclusions based on using these hydrides as model substrates can be misleading.[10f,27] For the transition structure for the oxidation of dimethyl sulfide (**4a**, Figure 4), both the RB3LYP solution at the B3LYP/6-311G** optimized geometry and the RHF solution at the MP2/6-31G* optimized geometry are triplet stable.[28] The syn-transition structure **4b** with the longer SO bond distance (Figure 4) has been found only at the MP2 level. The B3LYP geometry optimizations starting from **4b** led eventually to anti-transition structure **4a**. An IRC analysis[29] from the transition structure to products, DMSO and nitrous acid, showed that the 1,4 hydrogen shift to produce the neutral leaving group, HONO, occurred after the barrier was crossed in a manner shown previously for oxidation with peroxyformic acid.[10c] The transition structure **4b** is higher in energy than **4a** and the RHF solution for **4b** is triplet unstable. The RB3LYP solution for the transition structure (**5**) for the oxidation of trimethylamine with peroxynitrous acid is triplet stable.

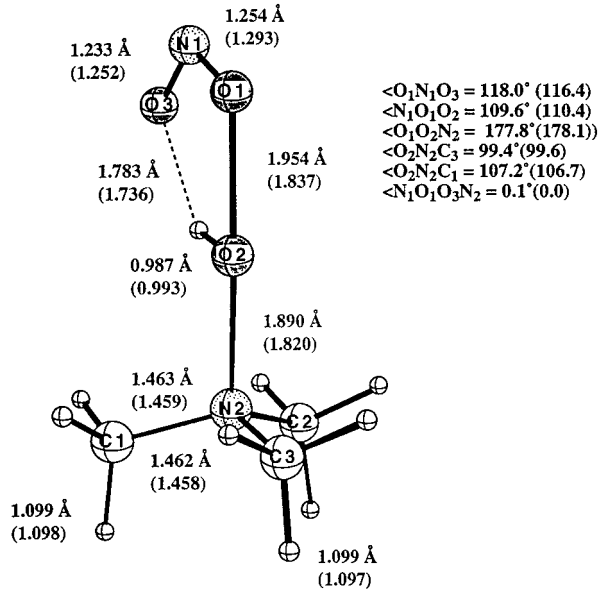

5

Figure 5. Geometrical parameters of transition structure **5a** for the oxidation of trimethylamine with peroxynitrous acid optimized at the B3LYP/6-311G** and MP2(full)/6-31G* (in parentheses) levels. The calculated activation barriers are given in Table 5.

While the nitrogen in transition structure **5** possesses a tetrahedral-type of bond configuration (Figure 5), the oxidation of trimethylphosphine with peroxynitrous acid leads to a bipyramidal-type transition structure **6** with the oxygen in an

(26) (a) Swern, D. *J. Am. Chem. Soc.* **1947**, *69*, 1692. (b) The relative rates of epoxidation of ethylene, propene, styrene, isobutene, and 2-butene with peracetic acid are 1, 22, 59, 484, and 489, respectively.

(27) Jaconbsen, H.; Berke, H. *Chem. Eur. J.* **1997**, *3*, 881.

(28) The lowest eigenvalues of the triplet stability matrixes ($^t\lambda_+$) are 0.01039 and 0.03150 hartree, respectively. It should be noted that while the B3LYP and MP2 optimized geometries of **4a** are close to each other, the RHF solution at the B3LYP/6-311G** geometry of transition structure **4a** shows a triplet instability ($^t\lambda_+ = -0.084012$ hartree).

(29) Gonzalez, C.; Schlegel, H. B. *J. Chem. Phys.* **1989**, *90*, 2154.

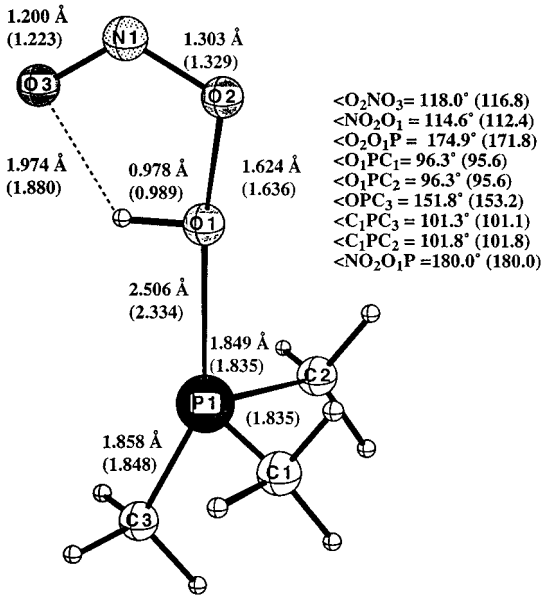

6

Figure 6. Geometrical parameters of transition structure **6** for the oxidation of trimethylphosphine with peroxynitrous acid optimized at the B3LYP/6-311G** and MP2(full)/6-31G* (in parentheses) levels. The calculated activation barriers are listed in Table 5.

axial position as an electronegative ligand (Figure 6). The geometries of the SMe_2 and NMe_3 fragments in transition structures **4a** and **5** are similar to the geometries of the isolated reactants. The main changes in the geometries of these transition structures when compared with the isolated reactants are elongations of the O−O bond lengths in the HO−ONO fragment (Figures 4 and 5) similar to the geometric features for the transition structures of the epoxidation of ethylene and propene with peroxynitrous acid (Figures 2 and 3). As seen from inspection of these geometry changes, there is no clear-cut correlation between the O−O bond elongation in the HO−ONO fragments of these transition structures and the barrier heights for oxidation reactions with peroxynitrous acid. For example, the O−O bond in transition structure **5** is elongated by 0.526 Å with respect to that in HOONO calculated at the B3LYP/6-311G** level, whereas the O−O bond elongation is much less (0.196 Å) in TS-**6**. However, in contrast to the smaller O−O bond elongation in TS-**6**, the activation barrier for the oxidation of trimethylphosphine with peroxynitrous acid is lower (0.5 kcal/mol at the QCISD(T)/6-31G*//B3LYP/6-311G** level, Table 5) than that for trimethylamine (5.3 kcal/mol). The MP2 calculated distances between the oxygen (O_3) and hydrogen atoms in transition structures **4a**, **5**, and **6** are only slightly shorter when compared with those in peroxynitrous acid. Furthermore, the B3LYP/6-311G** calculations of **4a** indicate an even longer O_3−H distance (1.886 Å) than in **1** (1.860 Å). Thus, the extent of how much the transition structure geometry facilitates the subsequent proton transfer that accompanies oxygen transfer is not related directly to the activation barriers.

Both the B3LYP and MP2 geometries of **4a**, **5**, and **6** calculated at these levels of theory are comparable (Figures 4−6). The B3LYP barrier heights are substantially lower than those found at the MP2, MP4, QCISD, and QCISD(T) levels of theory (Table 4). This is consistent with earlier observations that the B3LYP calculations give rise to underestimated barrier heights. The extension of the basis set from 6−311G** to the 6-311+G(3df,2p) basis set results in a barrier increase of only 0.9 kcal/mol (Table 4). As suggested previously, underestimates of these activation energies can be corrected by calculating the barriers at the QCISD(T) level using the B3LYP optimized geometries.[10g]

Table 4. Barrier Heights (kcal/mol) for the Oxidation of Dimethyl Sulfide with Peroxynitrous Acid Calculated at Various Computational Levels

method	B3LYP/ 6-311G** geometry[a] **4a**	MP2(full)/ 6-31G* geometry[a] **4a**	MP2(full)/ 6-31G* geometry[a] **4b**
B3LYP/6-311G**	1.8b	3.7	7.5
MP2(full)/6-31G*	9.1	8.4	13.4
MP4SDTQ	5.3	6.9	10.6
QCISD	15.3	14.8	19.0
QCISD(T)	8.3	9.6	13.4

[a] B3LYP and MP2 optimized geometries of the transition structures for the oxidation of dimethyl sulfide with peroxynitrous acid (**4a** and **4b**) are shown in Figure 4. [b] The B3LYP/6-311+G(3df,2p)//B3LYP/6-311+G(3df,2p) calculations give a barrier of 2.7 kcal/mol.

Table 5. Barrier Heights (kcal/mol) for the Oxidations of Trimethylamine and Trimethylphosphine with Peroxynitrous Acid Calculated at Various Computational Levels

method	B3LYP/6-311G** geometry[a]	MP2(full)/6-31G* geometry[a]
Trimethylamine + Peroxynitrous Acid		
B3LYP/6-311G**	1.3 (2.3)[b]	7.4
MP2(full)/6-31G*	7.4	5.2
MP4SDTQ	1.7	1.6
QCISD	11.1	11.2
QCISD(T)	4.6	5.3
Trimethylphosphine + Peroxynitrous Acid		
B3LYP/6-311G**	−1.9[c]	
MP2(full)/6-31G*		0.6[c]
MP4SDTQ	−0.2c	−0.1[c]
QCISD	3.9	5.5
QCISD(T)	0.5	1.5

[a] B3LYP and MP2 optimized geometries of the transition structure (**5**) for the oxidation of trimethylamine with peroxynitrous acid are shown in Figure 5. [b] The barrier with the ZPE corrections calculated at the B3LYP/6-311G** level. [c] The barriers given with respect to the isolated reactants can be negative although the central barriers relative to the prereaction complexes are, of course, positive.

The extent of the electron density transfer from XMe_3 (X = N and P) fragments in TS-**5** and TS-**6** can be estimated by means of their group charges. The natural population analysis (NPA)[30] charges calculated at the B3LYP level suggest that 0.490 electrons are transferred from the NMe_3 fragment in TS-**5** and 0.191 from the PMe_3 fragment in TS-**6**. The Wiberg bond index (WBI)[32] values calculated with the NPA/NBO[30] indicate stronger O−O bonding and weaker P−O bonding in **6** (WBI(O−O) = 0.694 and WBI(P−O) = 0.195) than the O−O bonding and N−O bonding in **5** (WBI(O−O) = 0.390 and WBI(N−O) = 0.434). The relative O−O bond elongation indexes calculated as (*R*(O−O)TS − *R*(O−O)HOONO/R(O−O)HOONO) 100% are 36.8% and 13.8% for TS-**5** and TS-**6**, respectively (using the B3LYP/6-311G** geometries, Figures 1, 5, and 6). All these data taken together show that the oxidation of trimethylphosphine with peroxynitrous acid proceeds via an earlier

(30) (a) Reed, A. E.; Curtiss, L. A.; Weinhold, F. *Chem. Rev.* **1988**, *88*, 899. (b) NPA charges in organic molecules have been shown to be satisfactory for the correlation of charges with changes in molecular structure.[31]

(31) Wiberg, K. B.; Rablen, P. R. *J. Comput. Chem.* **1993**, *14*, 1504.

(32) Wiberg, K. B. *Tetrahedron* **1968**, *24*, 1083.

Table 6. Comparison of the Calculated Barriers (kcal/mol) for the Oxidation of Alkenes, Dimethyl Sulfide, Trimethylamine, and Trimethylphosphine with Peroxynitrous Acid, Peroxyformic Acid, and Dimethyldioxirane (DMDO)

reactants	peroxynitrous acid (20.3)[a]	peroxyformic acid (46.9)[a]	DMDO
ethylene	18.3[b]	18.8[b]	19.4[c]
propene	15.5[b]	16.0[b]	
dimethyl sulfide	9.6 (6.9)[d]	6.6[e]	9.4[e]
trimethylamine	5.3 (1.6)[d]	0.9[e]	6.3[e]
trimethylphosphine	1.5 (−0.1)[d]	0.5[e]	1.0[e]

[a] The O−O bond energies (D_o) calculated[4] with G2 theory are given in parentheses. [b] At the QCISD(T)/6-31G*//QCISD/6-31G* level. [c] The barrier for the ethylene epoxidation with DMDO was calculated at the QCISD(T)//QCISD(full)/6-31G* level. The barrier for the ethylene oxidation with the parent dioxirane is lower (16.6 kcal/mol at the same level).[10g] [d] At the QCISD(T)/6-31G*//MP2/6-31G* level, the barriers calculated at the MP4/6-31G*//MP2/6-31G* level are shown in parentheses. The QCISD(T)/6-31G*//B3LYP/6-31G* barriers are given in Tables 4 and 5. [e] At the MP4/6-31G*//MP2/6-31G* level.[10f]

transition structure than the oxidation of trimethylamine. As a consequence, the gas-phase activation barrier for reaction 4 is lower than that for reaction 3. As noted elsewhere,[10f] the gas-phase intrinsic nucleophilicities of these three substrates are comparable, while their relative reactivities in the condensed phase are largely a consequence of solvation and relative basicity rather than the enhanced polarizability typically ascribed to third-row elements.

Comparison of the Oxidation Barriers for Peroxynitrous Acid, Peroxyformic Acid, and Dimethyldioxirane. The origin of the profound difference in the D_o(O−O) values in peroxynitrous and peroxyformic acids (20.3 and 46.9 kcal/mol at 0 K, respectively; calculated using G2 theory)[4] can be attributed to the relative stability of the two radicals arising from O−O bond cleavage (eq 5) where it is shown that the NO_2 radical is 22.5 kcal/mol more stable than the formyloxyl radical at the G2 level of theory.

$$HCO_2\ (^2B_2) + HONO_2 \rightarrow HCO_3H + NO_2\ (^2A_1) \qquad \Delta H(0K) = -22.5\ \text{kcal/mol} \quad (5)$$

While peroxynitrous acid has a lifetime of 1−3 s at neutral pH[2] and the half-life[33] of dimethyldioxirane can be estimated as 1−3 days,[34] peroxyformic acid is quite stable (its half-life is $\sim 10^8$ years).[35] Despite the pronounced differences in the stability of these oxidants and in their O−O bond energies, the oxidation barriers of ethylene, dimethyl sulfide, trimethylamine, and trimethylphosphine are all surprisingly close (Table 6).

While the D_o(O−O) in HOONO is less than one-half of that in peroxyformic acid,[4] the barriers for the epoxidation of ethylene and propene with HOONO (18.4 and 15.5 kcal/mol at the QCISD(T)/6-31G*//QCISD/6-31G* level, respectively) are almost the same as those for the epoxidation with peroxyformic acid (18.8 and 16.0 kcal/mol, Table 6). The absence of a correlation with the homolytic BDE's suggests that a heterolytic O−O bond cleavage is involved. Consistent with this suggestion the proton affinity (PA, at 0 K) of the putative HCO_2^- leaving group in HOO(C=O)H epoxidations is only 4.0 kcal/mol larger than the PA of the corresponding developing NO_2^- leaving group (eq 6, G2 theory), whereas the energy difference in the relative stabilities of the corresponding radicals is much larger (eq 5).

$$HCO_2^- + HNO_2 \rightarrow HCO_2H + NO^{2-} \qquad \Delta H(0K) = -4.0\ \text{kcal/mol} \quad (6)$$

Since the 1,4 proton shift producing the neutral HCO_2H and HNO_2 leaving groups takes place after the barrier is crossed, the relative stability of the developing anions influences the activation barriers. The HCO_2^- and NO_2^- anions are fairly close in stability and the corresponding activation barriers do not differ greatly. Thus, oxidation reactions involving such two-electron donor as alkenes or sulfides may involve an O−O bond cleavage that is more heterolytic in nature and reflect the stability of the developing anionic leaving group.

We conclude that the large differences in the O−O bond energies do not necessarily imply that the activation barriers must differ from each other. Similarly, the close values of the O−O BDE can coexist with large differences in the reactivity of the corresponding oxidants. For example, trifluroperoxyacetic acid has almost the same D_0(O−O) value (47.0 kcal/mol, G2(MP2)) as that of peroxyformic acid (47.7 kcal/mol)[4] but it is orders of magnitude more reactive as an oxygen donor.[36] Therefore, the correlation of the barrier heights with the O−O bond dissociation energies in the oxidants is not straightforward, if it exists at all, and the barriers are evidently governed by an interplay of various factors.

Our earlier calculations of the oxidation of sulfides, amines, and phosphines with peroxyformic acid have shown that the methyl substituents considerably decrease the barriers.[10f] This is a reflection of the higher HOMO of the substituted nucleophile and an earlier transition structure. A similar trend can be expected for the oxidations with peroxynitrous acid. Indeed, the B3LYP barriers for the oxidations of dimethyl sulfide (1.8 kcal/mol) and trimethylamine (1.3 kcal/mol) with peroxynitrous acid are significantly lower than those for the oxidation of hydrogen sulfide and ammonia (17.8 and 14.7 kcal/mol, respectively, at the B3LYP/6-31G*).[11b] The activation barriers for the oxidations of dimethyl sulfide and trimethylamine with peroxynitrous acid (6.9 and 1.6 kcal/mol, respectively, at the MP4/6-31G*//MP2/6-31G* level; Tables 4-6) are similar to the barriers of their oxidations with peroxyformic acid (6.6 and 0.9 kcal/mol, respectively, at the same level, Table 6).[10f] The barriers for oxidations with dimethyldioxirane[10h] are close to those for the peroxynitrous and peroxyformic acids in oxidations of sulfides, amines, and phosphines (Table 6). Therefore, the feasibility of the facile oxidation of methyl-substituted sulfides, amines, and phosphines by peroxynitrous acid should not be different from that for peroxyformic acid and dimethyldioxirane.

4. Conclusions

(1) The activation barriers for the alkene (ethylene and propene) epoxidations (18.4 and 15.5 kcal/mol at the QCISD(T)/6-31G*//QCISD/6-31G* level, respectively) and for the oxidations of dimethyl sulfide, trimethylamine, and trimethylphosphine (8.3, 4.6, and 0.5 kcal/mol at the QCISD(T)/6-31G*//B3LYP/6-311G** level, respectively) with peroxynitrous acid are similar to the barriers of their oxidations with peroxyformic acid. Therefore, alkene epoxidation and the oxidations of such

(33) Benson, S. W. *The Foundations of Chemical Kinetics*; McGraw-Hill: New York, 1960.

(34) (a) The thermal unimolecular rearrangement of dimethyldioxirane into its corresponding ester is a main pathway of dioxirane decomposition; the activation energy that was experimentally determined in solution is 23−25 kcal/mol.[34b] (b) Curci, R.; Dinoi, A.; Rubino, M. F. *Pure Appl. Chem.* **1995**, *67*, 811.

(35) ($t_{1/2} = \ln 2/k$); assuming a first-order rate constant for the O−O bond homolysis in peroxyformic acid and using the G2 calculated Gibbs free energy for the O−O bond cleavage (at 298 K).

(36) Hart, H. *Acc. Chem. Res* **1971**, *4*, 337.

methyl-substituted nucleophiles as sulfides, amines, and phosphines by peroxynitrous acid should be comparable to those for peroxyformic acid and should be quite feasible in biological systems.

(2) The transition structures for the epoxidation of ethylene and propene with peroxynitrous acid are symmetrical with equal or almost equal bond distances between the carbons of the double bond and the spiro oxygen. This symmetrical type of transition structure is similar to that found for the transition structures of alkene epoxidations with peroxyformic acid.

(3) If the RB3LYP solutions for the transition structures of the epoxidation of alkenes with peroxynitrous acid suffer from a triplet instability, the B3LYP calculations can lead to unsymmetrical transition structures, in contrast to the CISD and QCISD optimizations that resulted in symmetrical transition structures. While the CISD and QCISD methods should be used to provide the correct geometry of the transition structure in these cases, the calculated activation barriers are not very sensitive to the type of the transition structure. The activation barriers calculated at the QCISD(T) level with use of the B3LYP optimized geometries are very similar to those computed at the QCISD(T)//QCISD and QCISD(T)//CISD levels of theory. The geometries of the transition structures calculated at the QCISD and CISD levels are comparable.

(4) The B3LYP calculated barriers for oxidations of such alkenes as ethylene and propene, as well as of dimethyl sulfide, trimethylamine, and trimethylphosphine, are underestimated when compared with those calculated at QCISD(T)//QCISD levels. Much better agreement has been found when the barriers were calculated at the QCISD(T) level with use of the B3LYP geometry.

5. Summary

Perhaps the most surprising aspect of this study is that the three peroxides, peroxynitrous acid, peroxyformic acid, and dimethyldioxirane, have diverse O−O bond dissociation energies but yet similar activation barriers for oxygen atom transfer. Therefore, the correlation of the barrier heights with the O−O bond dissociation energies in the oxidants is not straightforward, if it exists at all, and the barriers are evidently governed by an interplay of various factors.

Acknowledgment. This work has been supported by the National Science Foundation (CHE 96-96216). We thank the National Center for Supercomputing Applications (Urbana, Illinois) and the Pittsburgh Supercomputing Center for generous amounts of computer time.

JA972518H